Optimal Design of a 6.78-MHz Wireless Battery Charging System Based on Average Power Loss

Ming Liu, Chen Zhao,
Univ. of Michigan-Shanghai Jiao Tong Univ. Joint Institute,
Shanghai Jiao Tong University,
Shanghai, P. R. China
Email: mikeliu@sjtu.edu.cn
zc437041363@sjtu.edu.cn

Jibin Song
College of Instrumentation and Electrical Engineering,
Jilin University,
Changchun, Jilin, P. R. China
Email: jbsongsjtu@gmail.com

Chengbin Ma*[1,2]
1. Univ. of Michigan-Shanghai Jiao Tong Univ. Joint Institute,
2. School of Mechanical Engineering,
Shanghai Jiao Tong University,
Shanghai, P. R. China
Email: chbma@sjtu.edu.cn

***Abstract*—High frequency wireless power transfer (WPT) such as working at megahertz (MHz) is widely considered to be a promising candidate for charging the lithium-ion batteries of the mobile electronic devices. However, in a real battery charging application, the varying battery voltage and charing current will significantly affect the system efficiency and lead to the high power losses in the whole charging process, especially at MHz. In order to reduce the power losses, a 6.78-MHz wireless battery charging system is proposed and an optimization design procedure is developed to minimize the average power loss in the whole charging process. By using the circuit model of the wireless battery charging system, the system efficiency is derived and services as the basis of the optimization design. Finally, the simulation results are provided for verification. It shows that the system using the proposed optimization design can achieve a 27.6% reduction of the average power loss compared with that using the conventional design method.**

***Index Terms*—Megahertz Wireless Battery Charging System, Lithium-ion Battery, Optimization, Power Loss**

I. Introduction

Wireless power transfer (WPT) using inductive resonance coupling is now being applied to charge various electronic devices and even electric vehicles [1], [2]. For large-power applications, WPT working at kilohertz (kHz) is making rapid progress particularly in terms of coil design and control [3]–[7]. In order to build more compact and lighter WPT systems, it is desirable to further increase operating frequency to several megahertz (MHz) such as 6.78 and 13.56 MHz. At the same time, a higher level of spatial freedom, namely a longer transfer distance and higher tolerance to coupling coil misalignment, can be achieved with the higher operating frequency. However, a major limitation is that the present power electronics devices can not afford the high power and the high operating frequency at the same time. Therefore, the MHz WPT is usually considered to be suitable for mid-range and low-power mobile consumer electronics [2], [8]–[10].

A practical challenge for MHz WPT systems is the high switching loss of the conventional hard-switching-based power amplifiers (PA) and rectifiers. The soft-switching-based ones are promising candidates to build high-efficiency MHz WPT systems, such as the Class E PA and rectifier. The Class E PA was first introduced for high-frequency applications in [11]. It has been applied in MHz WPT systems thanks to its high efficiency and simple structure [12], [13]. Similarly, the Class E rectifier has also been proposed for high-frequency rectification [14]. A high efficiency of the class E rectifier, 94.43%, was reported for an 800 kHz WPT system in [15]. Thus both the Class E PA and rectifier can be applied to achieve high-performance MHz wireless battery charging systems.

It is known that lithium-ion batteries are widely used in the consumer electronics due to its high performance [16]. The typical charging profile of the lithium-ion battery consists of two parts, the constant current (CC) mode and constant voltage (CV) mode. At the beginning of a charging cycle, the battery is charged in CC mode and the battery voltage increases. When the battery voltage reaches the nominal value, the charging system goes into the CV mode and the charging current drops rapidly. Considering the battery lifetime and recycle time, a wireless battery charging system should provide accurate charging current and voltage according to the battery charging profile [17].

In conventional WPT systems with the Class E PA and the Class E rectifier, the system parameters are optimized only for a specific target operating condition, namely fixed coil relative position and final load [18]. However, in the real battery charging applications, the varying final load, i.e., the varying battery voltage and charging current, will significantly affect the system efficiency and lead to the high power losses in the whole charging process, especially at MHz. Thus, this paper proposes a 6.78-MHz wireless battery charging system and an optimization design procedure with respect to the varying final load. In order to improve the system efficiency in the whole charging process, a L matching network is employed in the system to suppress the adverse effect of the varying load. The efficiency of the proposed battery charging system is derived by using batteries as the final load. Based on the charging system and the efficiency derivation, a parameter design procedure is developed for the battery charging system to optimize the average power loss in the whole charging process. The final simulation results validate the proposed 6.78-MHz wireless battery charging system and the parameters optimization design.

II. Fundamental Analysis

The circuit configuration of a typical 6.78-MHz wireless battery charging system is shown in Fig. 1. It consists of the power amplifier (PA), coupling coils, the rectifier, and the lithium-ion battery. Z_{in} is the input impedance of the coupling coils. Z_{out} is the input impedance seen from the receiving coil. In the wireless charging system, V_{bat} is the battery voltage and

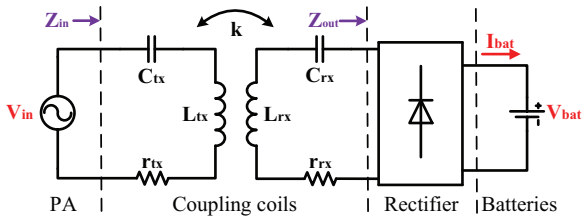

Fig. 1. Circuit configuration of a 6.78-MHz wireless battery charging system.

I_{bat} is the charging current. Fig. 2 shows a typical charging profile of the lithium-ion battery pack (4S1P) from SANYO (UR18650A). Here the constant charging current is 1A and the constant battery voltage is 16.8V. Due to the varying battery voltage and charging current, the impedance Z_{out} is varying with the battery charging profile.

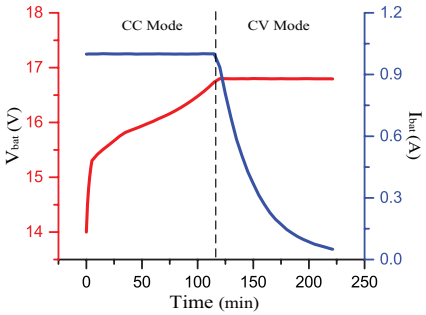

Fig. 2. A typical charging profile of the lithium-ion battery pack.

The performance of the 6.78-MHz wireless battery charging system is then investigated using a well-known RF circuit simulation software, the advanced design system (ADS) from Keysight. Fig. 3 (a) shows the simulation results of the resistance and reactance of Z_{out}, R_{out} and X_{out}, in the whole charge process. A Class E rectifier [refer to Fig. 5] is used in the simulation. It can be seen that the reactance X_{out} increases dramatically in the CV mode. The large reactance will significantly affect the efficiency of the coupling coils. Fig. 3 (b) shows the simulation results of the efficiency of the coupling coils. Here the parameters of the coupling coils given in table I is applied. It can be seen that the efficiency of the coupling coils decreases rapidly with the increasing reactance in the CV mode [refer to Fig. 3 (a)]. Fig. 4 gives the simulation results of the input impedance of the coupling coils. The resistance and the reactance of Z_{in}, R_{in} and X_{in}, decreases rapidly in the CV mode due to the increasing X_{out}. The small resistance of Z_{in} will lead to the high power losses

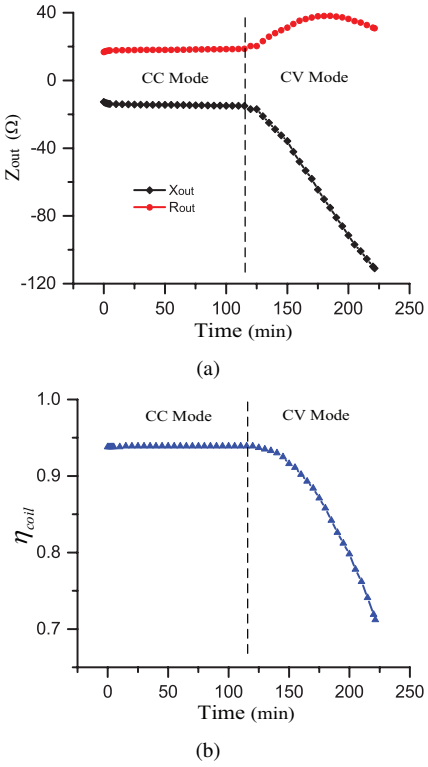

Fig. 3. Simulation results of the input impedance of the rectifier and the efficiency of the coupling coils. (a) Z_{out}. (b) η_{coil}.

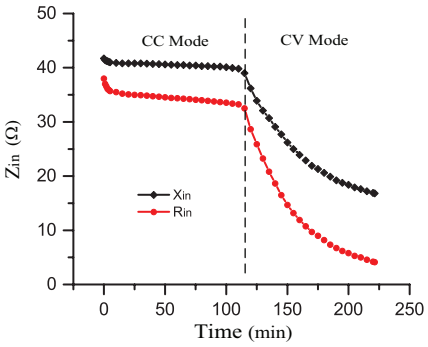

Fig. 4. Simulation results of the input impedance of the coupling coils Z_{in}.

TABLE I
Parameters of the coupling coils.

k	L_{tx}	L_{rx}	C_{tx}	C_{rx}	r_{tx}	r_{rx}
0.2	3.34 μH	3.34 μH	165 pF	165 pF	0.7 Ω	0.7 Ω

on the parasitic resistance of the components of the PA. Thus the increasing X_{out} also affects the PA efficiency.

Based on the above analysis, a 6.78-MHz wireless battery charging system is proposed to achieve the high overall efficiency and the low power losses in the whole charging process, as shown in Fig. 5. The Class E PA and rectifier are employed in the charging system due to their high efficiencies for high frequency applications. For the purpose of improving the overall efficiency in the whole charging profile, a L matching network is used to suppress the variations of Z_{out}. The L matching network consists of a series inductor L_s and

a parallel capacitor C_p. In the system, L_{dc} and L_f are the dc filter inductor of the Class E PA and rectifier, respectively. C_0 and C_s are the series and parallel capacitors of the Class E PA, respectively. C_{rx} is the compensation capacitor of the receiving coil L_{rx}. C_r is the shunt capacitor of the Class E rectifier. C_o is the dc output capacitor of the rectifier. Based on the proposed wireless battery charging system, the system efficiency with respect to the battery voltage and charging current is derived and an optimization design method for the system parameters is developed by using the derived system efficiency to optimize the average power loss in the whole charging process.

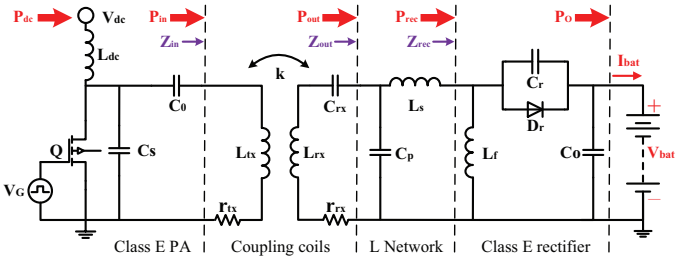

Fig. 5. The proposed 6.78-MHz wireless battery charging system.

III. Circuit Model and Efficiency Derivation

Fig. 6 shows the equivalent circuit model of the 6.78-MHz wireless battery charging system given in Fig. 5. In the circuit model, the dc filter inductors L_{dc} and L_f are equivalent to the resistances $r_{L_{dc}}$ and r_{L_f}, respectively. r_{L_s} is the equivalent series resistance (ESR) of the ac inductor L_s. r_Q is the on-resistance of the switch Q. V_f and r_{D_r} are the forward voltage drop and the on-resistance of the diode D_r. Z_{rec} is the input impedance of the Class E rectifier. R_{dc} is the equivalent resistance of the charging system shows to the dc power supply. I_{dc} and I_{BAT} are the dc input and output current of the charging system, respectively. i_{in} and i_{out} are the sinusoidal input and output current of the coupling coils, respectively. i_{rec} is the sinusoidal input current of the Class E rectifier. i_Q is the current in the switch when Q is on. Similarly i_{D_r} is the current that flows through the diode when D_r is on. According to [19], the following equations for the Class E rectifier in this charging system can be derived as

$$I_{m,rec} = -\frac{I_{bat}}{\sin\phi_1}, \tag{1}$$

$$\tan\phi_1 = \frac{1-\cos 2\pi D}{\sin 2\pi D + 2\pi(1-D)}, \tag{2}$$

$$\begin{aligned}\frac{2\pi\omega V_{bat}C_r}{I_{bat}} &= 1+\frac{[\sin 2\pi D+2\pi(1-D)]^2}{1-\cos 2\pi D}\\ &- 2\pi^2(1-D)^2-\cos 2\pi D,\end{aligned} \tag{3}$$

$$R_{rec} = \frac{2V_{bat}\sin^2\phi_1}{I_{bat}}, \tag{4}$$

$$X_{rec} = -\frac{1}{\pi}\left[\frac{a+b}{\omega C_r}\right], \tag{5}$$

$$a = \pi(1-D)+2\pi(1-D)\sin\phi_1\sin(\phi_1-2\pi D), \tag{6}$$

$$b = \sin 2\pi D+\frac{1}{4}\sin(2\phi_1-4\pi D)-\frac{1}{4}\sin 2\phi_1, \tag{7}$$

where ϕ_1 is the initial phase of i_{rec}, D is the duty cycle of the rectifier, ω is the operating frequency(6.78-MHz here), R_{rec} and X_{rec} are the resistance and reactance of Z_{rec}, $I_{m,rec}$ is the amplitude of i_{rec}, a and b are the intermediate variables. By using the law of conservation of energy, the following equation can be obtained

$$I_{m,out}^2 R_{out} = I_{m,rec}^2 R_{rec} + I_{m,rec}^2 r_{L_s}, \tag{8}$$

where $I_{m,out}$ is the amplitude of i_{out} and R_{out} is the equivalent resistance of Z_{out}. Based on the circuit model given in Fig. 6, the equivalent resistance and reactance of Z_{out}, R_{out} and X_{out}, can be derived as

$$R_{out} = \frac{R_{rec}+r_{L_s}}{(\omega C_p)^2[(R_{rec}+r_{L_s})^2+(\frac{1}{\omega C_p}+\omega L_s+X_{rec})^2]}, \tag{9}$$

$$X_{out} = \frac{(\omega C_p)(R_{rec}+r_{L_s})^2+(X_{rec}+\omega L_s)}{(\omega C_p)^2[(R_{rec}+r_{L_s})^2+(\frac{1}{\omega C_p}+\omega L_s+X_{rec})^2]}. \tag{10}$$

Substituting (1) into (8) gives

$$I_{m,out} = \frac{I_{bat}}{|\sin\phi_1|}\sqrt{\frac{R_{rec}+r_{L_s}}{R_{out}}}. \tag{11}$$

Similarly, by using the law of conservation of energy and the above eqautions, the amplitude of i_{out}, $I_{m,out}$, is derived as

$$I_{m,in} = \frac{I_{bat}}{|\sin\phi_1|}\sqrt{\frac{R_{rec}+r_{Ls}}{R_{out}}}\sqrt{\frac{R_{out}+r_{rx}}{R_{in}-r_{tx}}}, \tag{12}$$

where the equivalent resistance and reactance of Z_{in}, R_{in} and X_{in}, can be obtained as follows based on the circuit model.

$$R_{in} = r_{tx}+\frac{\omega^2 {L_m}^2(R_{out}+r_{rx})}{(R_{out}+r_{rx})^2+(X_{out}+\omega L_{rx}-\frac{1}{\omega C_{rx}})^2}, \tag{13}$$

$$X_{in} = \omega L_{tx}-\frac{\omega^2 {L_m}^2(X_{out}+\omega L_{rx}-\frac{1}{\omega C_{rx}})}{(R_{out}+r_{rx})^2+(X_{out}+\omega L_{rx}-\frac{1}{\omega C_{rx}})^2}. \tag{14}$$

L_m is the mutual inductance and it can be expressed as

$$L_m = k\sqrt{L_{tx}L_{rx}}, \tag{15}$$

where k is the mutual inductance coefficient. According to [20] and the circuit model, the following equations can be obtained.

$$I_{dc} = \frac{I_{m,in}}{g}, \tag{16}$$

$$R_{dc} = \frac{\pi^2-g(2\pi\cos\phi_2+4\sin\phi_2)}{4\pi\omega C_S}, \tag{17}$$

$$g = \frac{2\pi\sin(\varphi+\phi_2)+4cos(\varphi+\phi_2)}{4\cos\phi_2\sin(\varphi+\phi_2)+\pi\cos\varphi}, \tag{18}$$

$$\varphi = arc\tan\frac{X_{in}-\frac{1}{\omega C_0}}{R_{in}}, \tag{19}$$

$$\phi_2 = arc\tan\frac{\frac{\pi^2}{2}-4-\pi\omega C_S\left[2R_{in}+\pi(X_{in}-\frac{1}{\omega C_0})\right]}{\pi+\pi^2\omega C_S R_{in}-2\pi\omega C_S(X_{in}-\frac{1}{\omega C_0})}, \tag{20}$$

where R_{dc} is the equivalent resistance of the charging system shows to the dc power supply, ϕ_2 is initial phase of i_{in}, g and

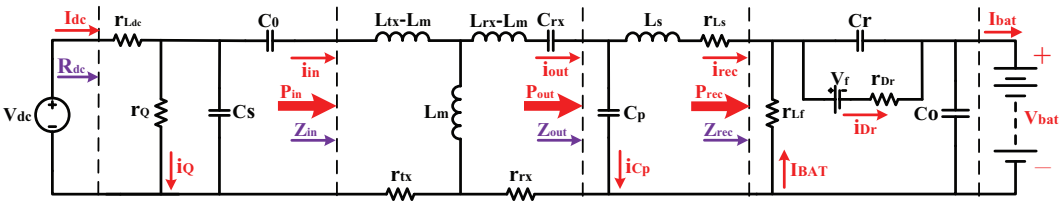

Fig. 6. Equivalent circuit model of the 6.78-MHz wireless battery charging system.

φ are the intermediate variables. Substituting (12) into (16) gives

$$I_{dc} = \frac{I_{bat}}{g\left|\sin\phi_1\right|}\sqrt{\frac{R_{rec}+r_{Ls}}{R_{out}}}\sqrt{\frac{R_{out}+r_{rx}}{R_{in}-r_{tx}}}. \quad (21)$$

For the simplifying purpose, the ESRs of the dc filter inductors(L_{dc} and L_f) and the parasitic parameters of the switch Q and the diode D_r are neglected in the above derivations. However, the power losses on them should be taken into consideration when deriving the system efficiency. Thus, the system efficiency can be expressed as

$$\eta_{sys} = \frac{I_{bat}V_{bat}}{I_{dc}^2R_{dc} + I_{dc}^2r_{L_{dc}} + I_{bat}^2r_{L_f} + P_{Q,loss} + P_{D_r,loss}}, \quad (22)$$

where

$$P_{Q,loss} = \frac{1}{2\pi}\int_0^{\pi} i_Q^2 r_Q d\omega t = \left(\frac{1}{2}+\frac{g}{\pi}+\frac{g^2}{4}\right)I_{dc}^2 r_Q, \quad (23)$$

$$\begin{aligned} P_{D_r,loss} &= \frac{1}{2\pi}\int_0^{2\pi D}(i_{D_r}^2 r_{D_r} + i_{D_r}V_f)d\omega t \\ &= eI_{bat}^2 r_{D_r} + fI_{bat}V_f, \end{aligned} \quad (24)$$

$$f = 2\pi + \cot\phi_1 - \frac{\cos(\phi_1 - 2\pi D)}{\sin\phi_1}, \quad (25)$$

$$\begin{aligned} e &= D + \frac{D}{2\sin^2\phi_1} - \frac{\cos(\phi_1-2\pi D)}{\pi\sin\phi_1} \\ &+ \frac{3\sin 2\phi_1 + \sin(2\phi_1 - 4\pi D)}{8\pi\sin^2\phi_1}. \end{aligned} \quad (26)$$

Substituting (21)(23)(24) into (22) gives (27). It can be seen from (27), the system efficiency depends on the battery voltage V_{bat}, the charging current I_{bat}, the parasitic parameters of the components, and the system parameters. Note the system parameters are included in R_{dc}, R_{in}, R_{out}, and R_{rec}.

IV. Design Parameters Optimization

As discussed in section II, the varying battery voltage and charging current significantly affect the performance of the wireless battery charging system. Based on the derivation of the system efficiency [refer to (27)], an optimization design method for system parameters is proposed to minimize the power losses in the whole charging process. In this approach, an average power loss with respect to the whole charging profile of the target battery pack is defined and used to optimize the system parameters. At a given time of the charging profile, t, the system output power can be expressed as

$$P_O(t) = I_{bat}(t)V_{bat}(t), \quad (28)$$

where $I_{bat}(t)$ and $V_{bat}(t)$ can be obtained from the charging profile of the battery pack [refer to Fig. 2]. Then, the power loss at the time t is

$$P_{loss}(t) = \frac{P_O(t)}{\eta_{sys}(t)} - P_O(t) = \frac{I_{bat}(t)V_{bat}(t)}{\eta_{sys}(t)}(1-\eta_{sys}(t)). \quad (29)$$

Here $\eta_{sys}(t)$ can be calculated by substituting $I_{bat}(t)$ and $V_{bat}(t)$ into (27). In order to obtain the average power loss in the whole charging process and use the numerical optimization to design the system parameters, the continuous charging profile of the battery pack is discretized into N points. It means that the entire charging time is averagely divided into N parts for the system power loss calculation. In this case, the objective function of the parameters optimization design, i.e., the average power loss, can be defined as

$$P_{avg,loss} = \frac{\sum_{i=1}^{N}\frac{I_{bat}(t_i)V_{bat}(t_i)}{\eta_{sys}(t_i)}(1-\eta_{sys}(t_i))}{N}. \quad (30)$$

It can be seen from (30), the average power loss includes the characteristics of the charging profile of the battery pack. In the charging system [refer to Fig. 5] and optimization design procedure, the inductor of the L matching network, L_s, is viewed as a constant parameter and C_p is the design parameter to be determined. C_0 and C_s are the design parameters of the Class E PA. For a more general discussion, the coupling coils are also viewed as the constant parameters in the optimization design of the charging system. But the compensation capacitor C_{rx} is taken as the design parameter and it is not pre-assumed to be resonant with the receiving coil. C_r is the design parameter for the Class E rectifier. Thus, the design parameters in the optimization design can be defined as

$$\mathbf{x} = [C_S, C_0, C_{rx}, C_p, C_r]. \quad (31)$$

where $\mathbf{x}$ is a vector representing the design parameters. The feasible range of $\mathbf{x}$ is defined as

$$\mathbf{x} \in (\mathbf{x}^{\mathbf{L}\cdot}, \mathbf{x}^{\mathbf{U}\cdot}), \quad (32)$$

where $\mathbf{x}^{\mathbf{L}\cdot}$ and $\mathbf{x}^{\mathbf{U}\cdot}$ are the lower and upper bounds of $\mathbf{x}$, respectively. The constant parameters in the optimization design of the charging system are

$$\mathbf{p_{con}} = [L_{tx}, L_{rx}, V_f, r_{D_r}, r_{L_1}, r_{tx}, r_{rx}, r_{L_r}, r_{L_f}, r_Q, \omega, k]. \quad (33)$$

Based on the above equations, the entire numerical optimization problem can be formulated as

$$\min_{\mathbf{x}} f(\mathbf{x}) = P_{avg,loss}(\mathbf{x}, \mathbf{p_{con}}, I_{bat}(t), V_{bat}(t)). \quad (34)$$

$$\eta_{sys} = \frac{4\pi V_{bat}}{\frac{[(R_{rec}+r_{Ls})(R_{out}+r_{rx})]\left[4\pi(R_{dc}+r_{L_{dc}})+(2+4g+\pi g^2)r_Q\right]}{R_{out}(R_{in}-r_{tx})g^2\sin^2\phi_1} + 4\pi\left[I_{bat}(r_{L_f}+er_{D_r})+fV_f\right]}. \quad (27)$$

It can be seen that the average power loss is determined by the design parameters, the constant parameters, $I_{bat}(t)$ and $V_{bat}(t)$. Since $I_{bat}(t)$ and $V_{bat}(t)$ are determined by the charging profile of the battery pack, the average power loss depends on the charging profile. The purpose of the optimization problem is to find an optimal set of the design parameters, $\mathbf{x_{opt}}$, that achieves the lowest average power loss ($P_{avg,loss}$) with respect to a specific charging profile. Given the nature of the optimization problem in (30)–(34), it is appropriate to apply genetic algorithm (GA), a popular population-based heuristic approach, to find a global or at least near-to-global optimal solution [5], [21].

V. Simulation Verification

An example simulation model is built up to validate the proposed 6.78-MHz wireless battery charging system and parameters optimization design by using the RF circuit simulation software, the advanced design system (ADS). The simulation system has a same configure as the one in Fig. 5, where the constant parameters $\mathbf{p_{con}}$ in Table II are applied. The Pspice models of the diode STPSC406 and the MOSFET SUD06N10 are used in the simulation.

TABLE II
Constant Parameters

ω	L_{tx}	L_{rx}	V_f	r_{D_r}	r_{L_1}
6.78 MHz	3.34 μ H	3.34 μ H	1.2 V	0.3 Ω	0.3 Ω
k	r_{tx}	r_{rx}	r_{L_r}	r_{L_f}	r_Q
0.2	0.7 Ω	0.7 Ω	0.2 Ω	0.2 Ω	0.225 Ω

In the optimization design, the feasible range of the design parameters, $\mathbf{x} = [C_S, C_0, C_{rx}, C_1, C_r]$, are given as

$$\mathbf{x^{L.}} = [100\text{ pF}, 100\text{ pF}, 100\text{ pF}, 100\text{ pF}, 100\text{ pF}],$$
$$\mathbf{x^{U.}} = [2000\text{ pF}, 2000\text{ pF}, 2000\text{ pF}, 2000\text{ pF}, 2000\text{ pF}]. \quad (35)$$

Here the feasible range are chosen based on the inductance of the coupling coils and the charging profile of the battery pack. By using the design procedure developed in section IV, the system efficiency derived in section III, and the charging profile given in Fig. 2, the optimal design parameters, $\mathbf{x_{opt}}$, are calculated as follows

$$\mathbf{x_{opt}} = [105\text{ pF}, 250\text{ pF}, 195\text{ pF}, 192\text{ pF}, 120\text{ pF}]. \quad (36)$$

Note in the above calculation, the number of discretization points, N, is chosen as 50. Based on the optimized system parameters, the simulation results in the whole charging process are given in the following. In the simulation, the CC mode and the CV mode of the charging profile given in Fig. 2 are achieved by tuning the dc input voltage of the charging system V_{dc} [refer to Fig. 5]. The corresponding dc input voltage of the charging system is given in Fig. 7. It can be seen that

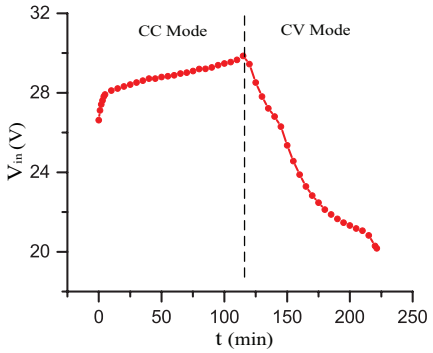

Fig. 7. Simulation results of the dc input voltage V_{dc}.

TABLE III
Optimized Results of Conventional Design

C_S	C_0	C_{rx}	C_r
130 pF	168 pF	165 pF	420 pF

V_{dc} increases in the CC mode and decreases rapidly when the charging process goes into the CV mode.

Fig. 8 and Fig. 9 give the simulation results of the system efficiency and power losses in the whole charging process, respectively. The simulation results of a 6.78-MHz WPT system using the conventional design method is also given for the comparison purpose. In this conventional design [18], the design parameters are optimized to let 1) resonance of the receiving coil at the target frequency, 6.78 MHz here; 2) ZVS operation of the Class E PA that maximizes the PA efficiency with respect to the specific Z_{in}, here Z_{in} at V_{bat} = 16.8 V and I_{bat} = 1 A; 3) a duty cycle D (=0.5) of the Class E rectifier, to lower the voltage stress on the rectifying diode [19]. Note the matching network is not used in the conventional design and the circuit model can be obtained from Fig. 5 by just removing the L matching network. Following these requirements, the optimized parameters of the conventional design are calculated and listed in Table III, based on a specific operating point of the charging profile, i.e., V_{bat} = 16.8V and I_{bat} = 1A at t = 115 min.

It can be seen from Fig. 8, the charging system using the optimization design can achieve the higher efficiency than that of the system using the conventional design in the whole charging process. It is because the optimization design method tends to improve the overall system efficiency in the whole charging process to minimize the average power losses of the charging system. As shown in Fig. 9, the wireless battery charging system using the optimization design can achieve the much lower power losses than that of the system using the conventional design in the whole charging process, which is consistent with the simulation results of the system efficiency. In order to validate the system efficiency derivation,

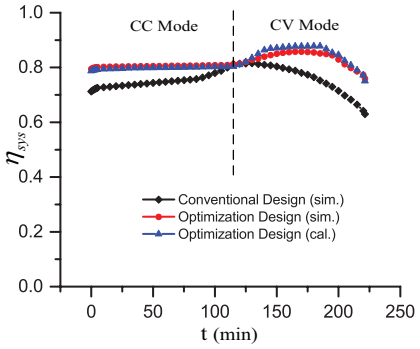

Fig. 8. Simulation results of the system efficiency.

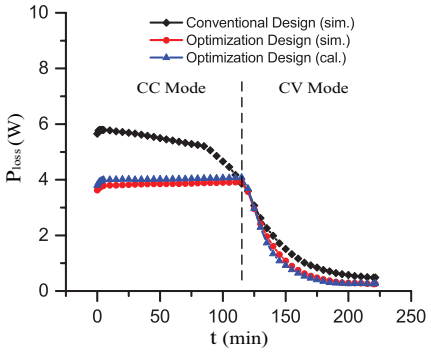

Fig. 9. Simulation results of the system power losses.

the calculation results are also given in Fig. 8 and Fig. 9. The good matching between the simulation and calculated results verifies the correctness of the equations of the system efficiency. Table IV lists the average power loss in the whole charging process. It can be seen that, by using the proposed optimization design method, the average power loss is lowered from 3.552 W to 2.573 W. The reduction of the average power loss is about 27.6%.

TABLE IV
SIMULATION RESULTS OF AVERAGE POWER LOSS

	Conventional Design	Optimization Design
Average Power Loss	3.552 W	2.573 W

VI. CONCLUSIONS

This paper proposes an optimization design of a 6.78-MHz wireless battery charging system to minimize the average power loss in the whole charging process. Based on fundamental analysis, a 6.78-MHz wireless battery charging system is proposed and the system efficiency is derived when using battery as the final load. Then a parameter design procedure is developed to optimize the average power loss of the charging system. Finally, the simulation results are given for verification. It shows that, by using the proposed optimization design, the wireless battery charging system can achieve a huge reduction (27.6%) of the average power loss compared with that using the conventional design method.

REFERENCES

[1] A. P. Sample, B. H. Waters, S. T. Wisdom, and J. R. Smith, "Enabling seamless wireless power delivery in dynamic environments," *Proc. IEEE*, vol. 101, no. 6, pp. 1343–1358, June Apr. 2013.

[2] S. Hui, W. Zhong, and C. Lee, "A critical review of recent progress in mid-range wireless power transfer," *IEEE Trans. Power Electron.*, vol. 29, no. 9, pp. 4500–4511, Sept 2014.

[3] N. Keeling, G. Covic, J. T. Boys *et al.*, "A unity-power-factor IPT pickup for high-power applications," *IEEE Trans. Ind. Electron.*, vol. 57, no. 2, pp. 744–751, Feb 2010.

[4] H. Li, K. W. Jie Li, W. Chen, and X. Yang, "A maximum efficiency point tracking control scheme for wireless power transfer systems using magnetic resonant coupling," *IEEE Trans. Power Electron.*, vol. 30, no. 7, pp. 3998–4008, July 2015.

[5] M. J. Neath, A. K. Swain, U. K. Madawala, and D. J. Thrimawithana, "An optimal pid controller for a bidirectional inductive power transfer system using multiobjective genetic algorithm," *IEEE Trans. Power Electron.*, vol. 29, no. 3, pp. 1523–1531, March 2014.

[6] W. Zhong and S. Hui, "Maximum energy efficiency tracking for wireless power transfer systems," *IEEE Trans. on Power Electron.*, vol. 30, no. 7, pp. 4025–4034, July 2015.

[7] J. Deng, W. Li, T. D. Nguyen, S. Li, and C. C. Mi, "Compact and efficient bipolar coupler for wireless power chargers: Design and analysis," *IEEE Transactions on Power Electronics*, vol. 30, no. 11, pp. 6130–6140, Nov 2015.

[8] M. Pinuela, D. C. Yates, S. Lucyszyn, and P. D. Mitcheson, "Maximizing DC-to-load efficiency for inductive power transfer," *IEEE Trans. Power Electron.*, vol. 28, no. 5, pp. 2437–2447, May 2013.

[9] W. Zhong, C. Zhang, X. Liu, and S. Hui, "A methodology for making a three-coil wireless power transfer system more energy efficient than a two-coil counterpart for extended transfer distance," *IEEE Trans. Power Electron.*, vol. 30, no. 2, pp. 933–942, Feb 2015.

[10] M. Fu, T. Zhang, C. Ma, and X. Zhu, "Efficiency and optimal loads analysis for multiple-receiver wireless power transfer systems," *IEEE Trans. Microw. Theory Tech.*, vol. 63, no. 3, pp. 801–812, March 2015.

[11] N. Sokal and A. Sokal, "Class E-A new class of high-efficiency tuned single-ended switching power amplifiers," *IEEE J. Solid-State Circuits*, vol. 10, no. 3, pp. 168–176, Jun 1975.

[12] S. Aldhaher, P.-K. Luk, A. Bati, and J. Whidborne, "Wireless power transfer using Class E inverter with saturable DC-feed inductor," *IEEE Trans. Ind. Appl.*, vol. 50, no. 4, pp. 2710–2718, July 2014.

[13] S. Aldhaher, P.-K. Luk, and J. F. Whidborne, "Electronic tuning of misaligned coils in wireless power transfer systems," *IEEE Trans. Power Electron.*, vol. 29, no. 11, pp. 5975–5982, Nov 2014.

[14] W. Nitz, W. Bowman, F. Dickens, F. Magalhaes, W. Strauss, W. Suiter, and N. Ziesse, "A new family of resonant rectifier circuits for high frequency DC-DC converter applications," in *Proc. Appl., Power Electron. Conf.*, New Orleans, LA, USA, Feb 1988, pp. 12–22.

[15] S. Aldhaher, P.-K. Luk, K. El Khamlichi Drissi, and J. Whidborne, "High-input-voltage high-frequency Class E rectifiers for resonant inductive links," *IEEE Trans. Power Electron.*, vol. 30, no. 3, pp. 1328–1335, March 2015.

[16] A. Khaligh and Z. Li, "Battery, ultracapacitor, fuel cell, and hybrid energy storage systems for electric, hybrid electric, fuel cell, and plug-in hybrid electric vehicles: State of the art," *IEEE Trans. Veh. Technol*, vol. 59, no. 6, pp. 2806–2814, July 2010.

[17] X. Qu, H. Han, S. C. Wong, C. K. Tse, and W. Chen, "Hybrid ipt topologies with constant current or constant voltage output for battery charging applications," *IEEE Trans. Power Electron.*, vol. 30, no. 11, pp. 6329–6337, Nov 2015.

[18] P.-K. Luk, S. Aldhaher, W. Fei, and J. Whidborne, "State-space modeling of a Class E^2 converter for inductive links," *IEEE Trans. Power Electron.*, vol. 30, no. 6, pp. 3242–3251, June 2015.

[19] M. Kazimierczuk, "Class E low dvd/dt rectifier," *Electric Power Applications, IEE Proceedings B*, vol. 136, no. 6, pp. 257–262, Nov 1989.

[20] M. Albulet, *RF power amplifiers*. SciTech Publishing, 2001.

[21] M. Li, S. Azarm, and A. Boyars, "A new deterministic approach using sensitivity region measures for multi-objective robust and feasibility robust design optimization," *Journal of mechanical design*, vol. 128, no. 4, pp. 874–883, Dec 2006.